Lipophilicity of amyloid β-peptide 12-28 and 25-35 to unravel their ability to promote hydrophobic and electrostatic interactions

International Journal of Pharmaceutics

Volume 495, Issue 1, 2015, Pages 179–185

DOI: 10.1016/j.ijpharm.2015.08.075

***Graphical Abstract (for review)**

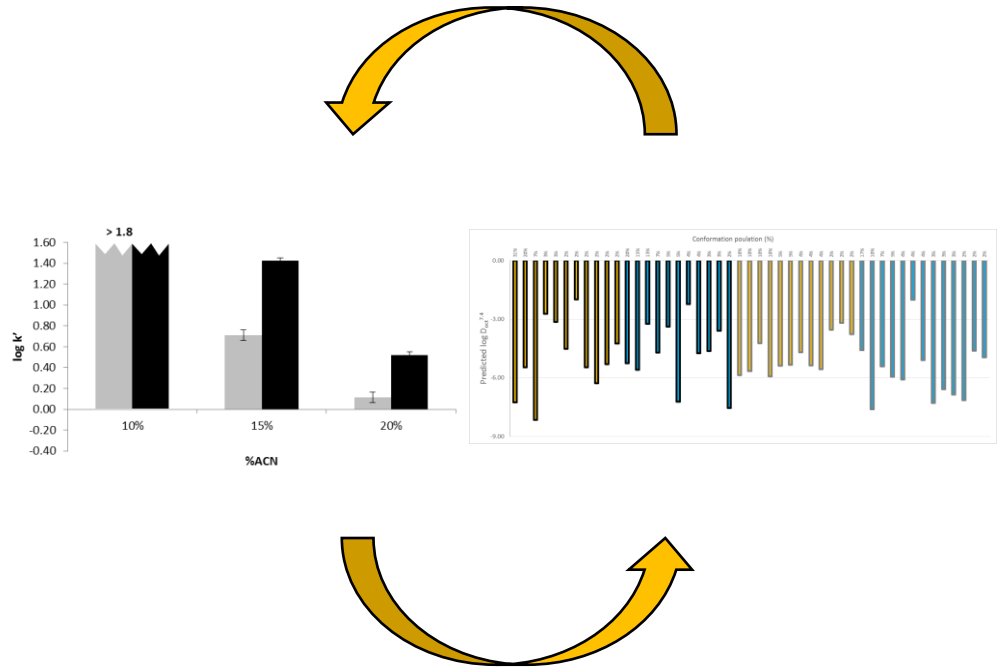

Lipophilicity of amyloid β-peptide 12-28 and 25-35 to unravel their skills to promote hydrophobic and electrostatic interactions

G. Ermondi[1], F. Catalano[2], M. Vallaro [1], I. Ermondi[1], M.P. Camacho Leal[1], L. Rinaldi[1], S. Visentin[1] and G. Caron[1]*

[1] *Molecular Biotechnology and Health Sciences Dept., Università degli Studi di Torino, via Quarello 15, 10135 Torino, Italy.*

[2] *Chemistry Dept., Università degli Studi di Torino, Via Giuria 5, 10125, Torino, Italy.*

E-mail: giulia.caron@unito.it, telephone: +39 011 6708337, fax: +39 011 2357282

Keywords

Amyloid peptide, circular dichroism, lipophilicity, molecular dynamics.

Abstract

The growing interest for peptide therapeutics calls for new strategies to determine the physico-chemical properties responsible for the interactions of peptides with the environment. This study reports about the lipophilicity of two fragments of the amyloid β-peptide, $A\beta_{25-35}$ and $A\beta_{12-28}$.

Firstly, computational studies showed the limits of log $D^{7.4}_{oct}$ in describing the lipophilicity of medium-sized peptides.

Chromatographic lipophilicity indexes (expressed as log k', the logarithm of the retention factor) were then measured in three different systems to highlight the different skills of $A\beta_{25-35}$ and $A\beta_{12-28}$ in giving interactions with polar and apolar environments. CD studies were also performed to validate chromatographic experimental conditions.

Results show that $A\beta_{12-28}$ has a larger skill in promoting hydrophobic and electrostatic interactions than $A\beta_{25-35}$. This finding proposes a strategy to determine the lipophilicity of peptides for drug discovery purposes but also gives insights in unraveling the debate about the aminoacidic region of Aβ responsible for its neurotoxicity.

1. Introduction

In recent years, peptide-based drug discovery has gained a lot of relevance because of good safety, tolerability and efficacy of peptides. Consequently, there is an important focus on new approaches to improve the use of peptides in pharmaceutical research (Otvos and Wade, 2014) (Fosgerau and Hoffmann, 2015).

Peptides behavior depends on their skill to interact with the environment (e.g. membranes and receptors) and on their aggregation properties. For instance, the amyloid β-peptide (Aβ, a peptide composed of 39−42 amino acids), is the most abundant component of β-amyloid plaques related to Alzheimer's disease (AD) (Hardy, 2009). Plaques formation is probably due to the skills of Aβ to form aggregates through the interaction with biomembranes (Wood et al., 2003)(Meier and Seelig, 2008)(Dies et al., 2014).

Lipophilicity studies provided a lot of information in the understanding of the interaction mechanisms between classical drugs (i.e. small organic compounds) and the environment (Testa et al., 1996) but poor information is reported in the literature about peptides.

We recently undertook a study to predict lipophilicity of small peptides (maximum length = 6 aminoacids) (Visconti et al., 2015). For these molecules, we found that they could be considered standard organic structures. However, the most relevant peptides in drug discovery are larger than six aminoacids and conformational effects are expected to strongly influence their behavior in the human body.

In this study, we characterize the lipophilicity of two flexible peptides of 11 and 17 aminoacids, respectively. In particular, we unravel the skills of two Aβ fragments, $A\beta_{25-35}$ and $A\beta_{12-28}$ in undertaking hydrophobic and polar interaction (the two main components of lipophilicity (El Tayar et al., 1992)) with polar and apolar environments. It should be recalled that shorter sequences of Aβ are often used as models of the full-length amyloid peptide, since they are easier to handle.

Computational studies were performed to highlight the limits of log $D^{7.4}_{oct}$ for characterizing the lipophilicity of the two medium-sized peptides.

Then we measured three chromatographic indexes (expressed as log k') using one reversed-phase (RP) and two Hydrophilic Interaction Chromatography (HILIC) (Buszewski and Noga, 2012) systems. The idea is to use two distinguished sets of chromatographic systems to catch the different skills of the two peptides to engage hydrophobic (RP) and electrostatic interactions (HILIC) with different environments. The determination of lipophilicity indexes by chromatography is supported by a number of advantages (e.g. small amounts of material are required, impurities can be separated during the measurements, there is no need for concentration determination, the process is fast and can be easily automated) (Poole and Poole, 2003).

CD studies were undertaken to validate some experimental settings used in the chromatographic determinations.

2. Material and methods

2.1 Materials

$A\beta_{12-28}$ and $A\beta_{25-35}$ were purchased from Polypeptide Laboratories France (Strasbourg, France, www.polypeptide.com).

1,1,1,3,3,3-Hexafluoro-2-propanol (HFIP), acetonitrile (ACN), dimethylsulfoxide (DMSO) and ammonium acetate were purchased from Alfa Aesar GmbH&Co (Karlsruhe, Germany, www.alfa.com).

Deionized water was used throughout.

2.2 Circular Dichroism

Solutions of $A\beta_{12-28}$ and $A\beta_{25-35}$ in the concentration range 30 - 400μM, both in pure HFIP and 10 mM PBS buffer at pH 7.4 + 10% HFIP, were scanned in the far-UV spectral range (four accumulations) over the wavelength region 180 - 260 nm with a scanning speed of 50 nm/min using a Jasco J-815 spectropolarimeter equipped with a Xe arc lamp. Spectra were recorded in a quartz

circular cuvette (optical path length 0.1 cm). Buffers baselines were subtracted for each measurement.

Secondary structure was estimated from the mean residue ellipticity [θ] with the CDNN CD spectra deconvolution software (Version 2.1, Copyright (C) 1997 Gerald Böhm).

2.3 Chromatography

The mobile phase consisted of 20 mM ammonium acetate buffer at pH 7.0 and acetonitrile in varying proportions. For all mobile phases, the given pH is the pH of the buffer before the addition of organic modifier.

The flow rate was 1 mL/min. The solvent front were used to determine t_0, i.e., the dead time in RP systems, toluene was used to determine t_0 under HILIC conditions.

HFIP solutions of both peptides were prepared (concentration range of 50-100 μg/mL) and injected in the HPLC systems. The choice of HFIP was made on the basis of preliminary tests, which evidenced the modest solubility of the two peptides in phosphate buffered saline (PBS) and DMSO. Conversely, they were largely soluble in HFIP.

The retention time (t_R) were measured on three columns: 1) PLRP-S polymeric reversed phase column (Agilent, 5cmx4.6mm, 5μm packing, 100Å pore size); 2) ZIC-HILIC column (sulfoalkylbetaine zwitterionic phase on a silica gel support, 10 cm × 4.6 mm, 5μm packing, 200Å pore size) from SeQuant (Umeå, Sweden) and 3) ZIC-cHILIC column (phosphorylcholine zwitterionic phase on a silica gel support, 10 cm × 4.6 mm, 3μm packing, 100Å pore size) from SeQuant (Umeå, Sweden). Measures were performed in triplicate.

The chromatographic indexes are expressed as log k' (Eq. 1)

$$log\ k' = log\ ((t_R - t_0)/t_0) \qquad Eq.\ 1$$

where k' is the retention factor, t_R is the retention time and t_0 is the dead time.

A HPLC Varian ProStar instrument equipped with a 410 autosampler, a PDA 335 LC Detector and Galaxie Chromatography Data System Version 1.9.302.952 was used.

2.4 Ionization and calculated lipophilicity

Ionization constants were calculated with MoKa (Version 2.5.4, *http://www.moldiscovery.com*); log $D^{7.4}_{oct}$ values were calculated with a model recently published by some of us (Visconti et al., 2015).

2.5 Molecular Dynamics simulations

All simulations and analysis described below were done using the AMBER14 package that also includes the trajectory analysis software AmberTools and the module xLEaP used to prepare starting structures (Case et al., 2012). In particular, MM minimizations and MD simulations were performed using sander and pmemd modules, respectively.

The starting structures of $A\beta_{12-28}$ and $A\beta_{25-35}$ were obtained from the crystallographic structure of $A\beta_{1-42}$ (PDB id: 1IYT) after deleting unnecessary aminoacids. MD simulations were performed with constant protonation states for titrable residues. Peptides were modeled in the electrical state dominating at pH = 7.0. Histidine was considered neutral and the ε-tautomer was used in the simulations according to default AMBER choice and to MoKa prediction.

Input files were prepared submitting all starting structures to the xLEaP module. The ff99SB force field was employed.

During the chromatographic experiments, peptides experience different environments that depend on the eluent composition. To obtain reliable simulations we tried to approach the experimental conditions used to register chromatograms. In particular, we considered two limit conditions. In the first, epsilon was fixed at 78.5 to mimic an aqueous environment. The second epsilon was set at 37.5 to mimic acetonitrile. Solvation effects for the investigated solvents (water and acetonitrile) were incorporated using the pairwise Generalized Born model with parameters described by Tsui and Case (Tsui and Case, 2000). This model uses the default radii set up by xLEaP.

Before launching MD simulations, all atoms were optimized without any constrain (500 cycles of steepest descent followed by 500 cycles of conjugate gradient minimization). After minimization, all systems were gradually heated from 0 to 325 K with a time step of 0.5 fs over a period of 35 ps. The temperature plot was used to confirm the attainment of the equilibrium of the heating phase. Finally, 50 ns MD simulations were performed with a time step of 2 fs. During the MD simulations, the atom coordinates were saved every 500 steps. All the covalent bonds involving hydrogen atoms were constrained with the SHAKE algorithm and the Berendsen thermostat was used, both as implemented in AMBER14. For temperature control a heat bath coupling of 1.0 ps and 0.5 ps were used during heating and MD simulation, respectively.

The MD Movie tool of USCF Chimera (Version 1.10, *http://www.cgl.ucsf.edu/chimera*) was used to cluster the trajectories based on pairwaise best-fit root-mean-square deviations (RMSDs) calculated on the backbone atoms and to identify a representative frame for each cluster. For any peptide we considered those clusters that taken together include about 80% of the entire population of conformers.

For validation purposes it should be mentioned that the most stable structure of $A\beta_{1-42}$ obtained with our approach (data not shown) is in agreement with that reported in the literature (Kobayashi and Takahashi, 2010). This result represents therefore an indirect validation of the applied computational method.

Processing was done on a two 8 cores Xeon E5 at 3.3GHz CPUs and 128GB of RAM.

3. Results and discussion

3.1 Ionization

The 2D chemical structures of $A\beta_{12-28}$ an $A\beta_{25-35}$ are shown in Figure 1. $A\beta_{12-28}$ has five basic centers and three acidic centers. All but histidine residues are fully ionized at physiological pH (in blue basic centers and in red acidic groups, Figure 1). $A\beta_{25-35}$ bears two basic (in blue) and one acidic (in red) groups, completely ionized at pH = 7.0. Summing up, at pH = 7.0 the net charge of $A\beta_{12-28}$ is 0 (three positive and three negative charges), whereas the net charge of $A\beta_{25-35}$ is +1 (two positive and one negative charges).

Please insert Figure 1 here

3.2 Lipophilicity

The most commonly used measure of lipophilicity is log $D^{7.4}_{oct}$. Calculation of Log $D^{7.4}_{oct}$ of the two peptides could be determined using a tool recently reported in the literature by some of us (Visconti et al., 2015). Since the method uses as an input the 3D structure of the investigated peptide, MD simulations of the monomeric form of $A\beta_{12-28}$ and $A\beta_{25-35}$ were performed in two environments (polar and apolar, see the MD simulations Section for more details) and some representative conformers were identified through cluster analysis. In particular, 11 conformers were retained for $A\beta_{12-28}$ in both environments whereas 12 and 13 conformers were considered for $A\beta_{25-35}$ in apolar and polar media, respectively.

All the representative conformations were submitted to the aforementioned tool (Visconti et al., 2015) to predict log $D_{oct}^{7.4}$. Results are summarized in Figure 2.

Please insert Figure 2 here

Predicted log $D_{oct}^{7.4}$ in Figure 2 outline that both peptides are very hydrophilic and thus their log $D_{oct}^{7.4}$ may be experimentally inaccessible through standard experimental techniques (e.g. shake-flask, potentiometry). Please note that when calculated log $D^{7.4}_{oct}$ are considered, caution should be exercised since the model on which the prediction is based was developed using a dataset of small peptides (Visconti et al., 2015).

Moreover, data in Figure 2 show that log $D_{oct}^{7.4}$ is strongly dependent on conformational changes in both environments (apolar=yellow; polar=cyan). This represents a major issue in the prediction of log $D_{oct}^{7.4}$ of investigated peptides but it is also expected that this result could be generalized and extended to most medium-sized peptides.

The limits of prediction called for experimental determinations. In particular, we measured the lipophilicity of $A\beta_{12\text{-}28}$ and $A\beta_{25\text{-}35}$ using a set of chromatographic lipophilicity indexes.

The determination of chromatographic lipophilicity indexes is widely applied to small organic molecules. The application to peptides is less common and thus some precautions were taken. In particular, since peptides could form aggregates, HFIP solutions of both samples were injected in the HPLC systems (see CD measurements).

Three chromatographic systems which show a different predominant mechanism of interaction with the solutes (Ermondi and Caron, 2012) were selected. Their main features are reported in Table 1.

The PLRP-S is a reversed phase (RP) system and thus solutes retention is mostly due to hydrophobic interactions between the solutes and the system (Ermondi and Caron, 2012). On the contrary, the HILIC systems, which are characterized by zwitterionic stationary phases, are expected to mainly describe electrostatic, polar and hydrogen bond (HB) interactions (Ermondi and Caron, 2012). Moreover, to get more specific information in the nature of electrostatic interactions, we used two HILIC systems which differ in the spatial orientation of the positive and negative charged groups (Di Palma et al., 2011).

Please insert Table 1 here

Retention factors were firstly determined using the polymeric PLRP-S column with a mobile phase containing small quantities of ACN due to the high polarity of the two peptides (Figure 3A). To obtain the maximum retention under RP conditions, the most non-polar available column should be used and thus we preferred the PLRP-S to either C8 or C18 columns. Under these conditions the log k' value of $A\beta_{12\text{–}28}$ is larger than that of $A\beta_{25\text{–}35}$ (Figure 3A). This is an expected result since $A\beta_{12\text{–}28}$ is larger than $A\beta_{25\text{–}35}$ in any environment (see MD results, Figure S1 in the Supplementary Material)

and thus should be retained more by a RP system whose retention is predominantly due to hydrophobicity (Ermondi and Caron, 2012).

In RP systems we expect that log k' decreases when the amount of organic solvent in the mobile phase increases. This was verified as shown in Figure 3A. An additional increase of the amount of acetonitrile in the mobile phase cannot be checked since under these experimental conditions the two peptides elute together with the solvent front ($t_0 = t_R$).

Please insert Figure 3 here

In order to characterize peptides polar properties, peptides retention was also determined using direct chromatographic systems (i.e. the HILIC and C-HILIC systems, see Table 1). This is a crucial step which distinguishes strategies for determining lipophilicity of peptides from those applied to small organic molecules. Peptides in fact are generally more ionized than classical drugs and thus have more propensity to form electrostatic interaction with the environment. This feature has to be determined with polar systems.

Figure 3B and 3C show that $A\beta_{12-28}$ is more retained on the HILIC columns than $A\beta_{25-35}$. This could be ascribed to the larger number of ionized centers present on $A\beta_{12-28}$, which favor the interaction with the zwitterionic moiety present on the column surface.

The recently developed C-HILIC system differs from the HILIC for the structure and orientation of the zwitterionic group present on the stationary phase (Table 1). These structural differences should permit to discriminate positively from negatively charged compounds. $A\beta_{25-35}$ has an excess of positive charges and thus we expected that it has a larger affinity for the HILIC system in which the negative charge is more accessible than the positive one. Unexpectedly, results show that the C-HILIC system provides similar information than the HILIC system suggesting that the peptides interaction with HILIC and C-HILIC depends on a complex balance of factors not simply due to the number and nature of molecular charges but also on conformational effects. Additional studies are in progress to generalize this finding.

Taken together chromatographic data show that $A\beta_{12-28}$ has a larger skill to interact with both apolar and polar environments than $A\beta_{25-35}$.

3.3 Circular dichroism (CD) studies

CD studies were undertaken to unravel a) the influence of HFIP on the solutions injected in the HPLC systems and b) the propensity of the two peptides to self-aggregation.

The effect of HFIP on the secondary structure of peptides and proteins is largely controversial in the literature. Some reports attribute to HFIP a denaturing effect (Wei and Shea, 2006) whereas others consider such non-polar organic solvent (ε = 16.7) a disaggregating agent or an inductor and stabilizer of α-helix structures (Yanagi et al., 2011) (Ryan et al., 2013).

Increasing concentrations (30, 125, 250 and 400 μM) of both peptides were dissolved in pure HFIP and in PBS at pH 7.4 added with 10% v/v of HFIP (hereafter called PBS_{HFIP}). Solutions were analyzed by CD immediately after their preparation (Figure 4 and 5, panel A and B). PBS_{HFIP} solutions were also submitted to CD analysis 24h after preparation (Figure 4 and 5, panel C).

The CD profiles of $A\beta_{12-28}$ (Figure 4A and B) and $A\beta_{25-35}$ (Figure 5A and B) in PBS_{HFIP} are completely different from those registered in HFIP. In particular, HFIP favors unordered conformations. The PBS buffer seems to better stabilize ordered conformations of both peptides, favoring an increase of α-helices and β-sheet structures (more details about interpretation of CD spectra are reported in the Supplementary Material).

Please insert Figure 4 here

Please insert Figure 5 here

Self-aggregation phenomena could be present under chromatographic conditions where peptides concentration was about 400 μM. CD spectra analysis also reveals a substantial difference between the two analyzed samples after 24 hours (Figures 4 and 5, panel C): while the $A\beta_{12-28}$ tends to form agglomerates marked by the increase in intermolecular β-sheets, the $A\beta_{25-35}$ amyloid maintains a shape of the spectra indicative of a very high percentage of disordered structures. These results suggests that $A\beta_{12-28}$ has a higher propensity to self-assembly than $A\beta_{25-35}$. To avoid self-aggregation, chromatograms were obtained immediately after samples preparation.

4. Conclusion

This study provides some general guidelines about the determination of the lipophilicity of medium-sized peptides. In particular, we evidenced that peptides lipophilicity cannot be properly determined by traditional descriptors such as log $D_{oct}^{7.4}$ for two main reasons: a) peptides are too polar and thus log $D_{oct}^{7.4}$ is experimentally inaccessible, b) predictions of log $D_{oct}^{7.4}$ are unreliable because of the peptides conformational variability. Moreover, lipophilicity varies with the

environment and thus the octanol/water system is insufficient to mimic the different biological conditions.

To overcome these limits and to determine the physico-chemical profile of peptides for drug discovery purposes a set of three chromatographic descriptors have been proposed. In particular, we characterized the lipophilicity of $A\beta_{12-28}$ and $A\beta_{25-35}$ under RP, HILIC and C-HILIC conditions. Taken together log k' data showed that $A\beta_{12-28}$ has a larger skill to interact with hydrophobic and polar media than $A\beta_{25-35}$. Moreover, the two HILIC systems provided similar log k' values for $A\beta_{12-28}$ and $A\beta_{25-35}$. This was an unexpected result for $A\beta_{25-35}$ since its net charge is +1 and thus a larger retention on the HILIC than on the C-HILIC column was expected.

Since $A\beta_{12-28}$ and $A\beta_{25-35}$ are used as models of the amyloid peptide, these results definitively may improve the understanding of Aβ neurotoxicity, which originates from its interaction with lipid membranes. In general terms, the interaction of compounds with biomembranes is driven by two main mechanisms. The first is due to hydrophobic interactions with the alkyl chains of phospholipids, whereas the second is related to electrostatic interactions with their polar heads (van Balen et al., 2004). Since we proved that $A\beta_{12-28}$ has more propensity to form both types of interactions, the region of Aβ comprised between residues 12 and 28 is expected to be the responsible for the toxicity of the whole peptides. This contributes to unravel the discussion reported in the literature about this topic (Liu et al., 2004).

Acknowledgement

This work has been supported by Ateneo Compagnia di San Paolo-2012-Call 2, LIMPET project.

References

Buszewski, B., Noga, S., 2012. Hydrophilic interaction liquid chromatography (HILIC)--a powerful separation technique. Anal. Bioanal. Chem. 402, 231–47. doi:10.1007/s00216-011-5308-5

Case DA, Darden TA, Cheatham TE, Simmerling CL, Wang J, Duke RE, Luo R, Walker RC, Zhang W, Merz KM, Roberts B, Hayik S, Roitberg A, Seabra G, Swails J, Goetz AW, Kolossváry I, Wong KF, Paesani F, Vanicek J, Wolf RM, Liu J, Wu X, Brozell SR, Steinbrecher T, Gohlke H, Cai Q, Ye X, Wang J, Hsieh MJ, Cui G, Roe DR, Mathews DH, Seetin MG, Salomon-Ferrer R, Sagui C, Babin V, Luchko T, Gusarov S, Kovalenko A, Kollman, PA. AMBER 12. University of California, San Francisco. (2012).

Di Palma, S., Boersema, P.J., Heck, A.J.R., Mohammed, S., 2011. Zwitterionic hydrophilic interaction liquid chromatography (ZIC-HILIC and ZIC-cHILIC) provide high resolution separation and increase sensitivity in proteome analysis. Anal. Chem. 83, 3440–3447. doi:10.1021/ac103312e

Dies, H., Toppozini, L., Rheinstädter, M.C., 2014. The interaction between amyloid-β peptides and anionic lipid membranes containing cholesterol and melatonin. PLoS One 9(6), e99124. doi:10.1371/journal.pone.0099124

El Tayar, N., Tsai, R.S., Carrupt, P.-A., Testa, B., 1992. Octan-1-ol–water partition coefficients of zwitterionic α-amino acids. Determination by centrifugal partition chromatography and factorization into steric/hydrophobic and polar components. J. Chem. Soc., Perkin Trans. 2 79–84. doi: 10.1039/P29920000079

Ermondi, G., Caron, G., 2012. Molecular interaction fields based descriptors to interpret and compare chromatographic indexes. J. Chromatogr. A 1252, 84–9. doi:10.1016/j.chroma.2012.06.069

Fosgerau, K., Hoffmann, T., 2015. Peptide therapeutics: current status and future directions. Drug Discov. Today 20, 122–128. doi:10.1016/j.drudis.2014.10.003

Hardy, J., 2009. The amyloid hypothesis for Alzheimer's disease: A critical reappraisal. J. Neurochem. 110, 1129–1134. doi:10.1111/j.1471-4159.2009.06181.x

Kelly S.M., Jess T.J., Price N.C.; 2005. Biochim. Biophys. Acta. 1751, 119-139. doi:10.1016/j.bbapap.2005.06.005

Kobayashi, K., Takahashi, O., 2010. Molecular-Dynamics Simulations for Amyloid β 1 – 42 Monomer with d-Aspartic Acid Residues Using Continuous Solvent. Chem. Biodivers. 7, 1357–1363. doi: 10.1002/cbdv.200900299

Liu, R., McAllister, C., Lyubchenko, Y., Sierks, M.R., 2004. Residues 17-20 and 30-35 of Beta-Amyloid Play Critical Roles in Aggregation. J. Neurosci. Res. 75, 162–171. doi:10.1002/jnr.10859

Meier, M., Seelig, J., 2008. Length Dependence of the Coil - β -Sheet Transition in a Membrane Environment. Biochemistry 1017–1024. doi: 10.1021/ja077231r

Otvos, L., Wade, J.D., 2014. Current challenges in peptide-based drug discovery. Front. Chem. 2, 8–11. doi:10.3389/fchem.2014.00062

Poole, S.K., Poole, C.F., 2003. Separation methods for estimating octanol–water partition coefficients. J. Chromatogr. B 797, 3–19. doi:10.1016/j.jchromb.2003.08.032

Ryan, T.M., Caine, J., Mertens, H.D.T., Kirby, N., Nigro, J., Breheney, K., Waddington, L.J., Streltsov, V. a, Curtain, C., Masters, C.L., Roberts, B.R., 2013. Ammonium hydroxide treatment of Aβ produces an aggregate free solution suitable for biophysical and cell culture characterization. PeerJ 1, e73. doi:10.7717/peerj.73

Testa, B., Carrupt, P.-A., Gaillard, P., Tsai, R.S., 1996. Intramolecular Interactions Encoded in Lipophilicity: Their Nature and Significance, in: Pliska, V., Testa, B., van de Waterbeemd, H. (Eds.), Lipophilicity in Drug Action and Toxicology. Wiley-VCH Verlag GmbH & Co. KGaA, pp 49-71.

Tsui, V., Case, D. a., 2000. Theory and applications of the Generalized Born solvation model in macromolecular simulations. Biopolymers 56, 275–291. doi:10.1002/1097-0282(2000)56:4<275::AID-BIP10024>3.0.CO;2-E

Van Balen, G.P., Martinet, C. a M., Caron, G., Bouchard, G., Reist, M., Carrupt, P.-A., Fruttero, R., Gasco, A., Testa, B., 2004. Liposome/water lipophilicity: methods, information content, and pharmaceutical applications. Med. Res. Rev. 24, 299–324. doi:10.1002/med.10063

Visconti, A., Ermondi, G., Caron, G., Esposito, R., 2015. Prediction and interpretation of the lipophilicity of small peptides. J. Comput. Aided. Mol. Des. 29, 361–370. doi:10.1007/s10822-015-9829-4

Wei, G., Shea, J., 2006. Effects of Solvent on the Structure of the Alzheimer Amyloid- b (25 – 35) Peptide 91, 1638–1647. doi:10.1529/biophysj.105.079186

Wood, W.G., Eckert, G.P., Igbavboa, U., Müller, W.E., 2003. Amyloid beta-protein interactions with membranes and cholesterol: Causes or casualties of Alzheimer's disease. Biochim. Biophys. Acta - Biomembr. 1610, 281–290. doi:10.1016/S0005-2736(03)00025-7

Yanagi, K., Ashizaki, M., Yagi, H., Sakurai, K., Lee, Y., Goto, Y., 2011. Hexafluoroisopropanol Induces Amyloid Fibrils of Islet Amyloid Polypeptide by Enhancing Both Hydrophobic and Electrostatic Interactions * □ 286, 23959–23966. doi:10.1074/jbc.M111.226688

Figure Captions

Figure 1. The chemical structures of the two peptides. Acidic centers ionized at pH=7.0 are in red whereas basic centers ionized at the same pH are in blue. A) $A\beta_{12-28}$ and B) $A\beta_{25-35}$.

Figure 2. Predicted log $D^{7.4}_{oct}$ of the representative conformers resulting from MD simulations performed in the two different environments that mimic acetonitrile (ε=37.5 in cyan) and water (ε=78.5 in yellow) solvent, respectively. $A\beta_{12-28}$ is in black, $A\beta_{25-35}$ is in grey.

Figure 3. Lipophilicity data. $A\beta_{12-28}$ is in black, $A\beta_{25-35}$ is in grey. A) PLRP-S, B) HILIC, C) C-HILIC.

Figure 4. CD spectra of $A\beta_{12-28}$ in pure HFIP A), in PBS_{HFIP} B) and in PBS_{HFIP} 24 h after samples preparation C) are reported in the top panels at increasing concentration 30, 150, 250 and 400μM (corresponding to lines a, b, c and d respectively). CD spectra of pure secondary structures as indicated in literature (α-helix, β-sheet, turns and random coils corresponding to lines α, β, t and rc respectively) are reported in the bottom panels for the sake of a qualitative comparison (Kelly et al. 2005).

Figure 5. CD spectra of $A\beta_{25-35}$ in pure HFIP A), in PBS_{HFIP} B) and in PBS_{HFIP} 24 h after samples preparation C) are reported in the top panels at increasing concentration 30, 150, 250 and 400μM (corresponding to lines a, b, c and d respectively). CD spectra of pure secondary structures as indicated in literature (α-helix, β-sheet, turns and random coils corresponding to lines α, β, t and rc respectively) are reported in the bottom panels for the sake of a qualitative comparison (Kelly et al. 2005).

Table 1

Table 1. Features of the four chromatographic systems used in the paper

Name	Type	Stationary phase	Interaction
PLRP-S	reversed	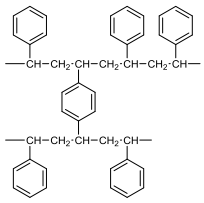	hydrophobic
HILIC	direct	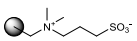	ionic
C-HILIC	direct	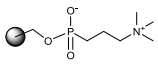	ionic

Figure 1

A

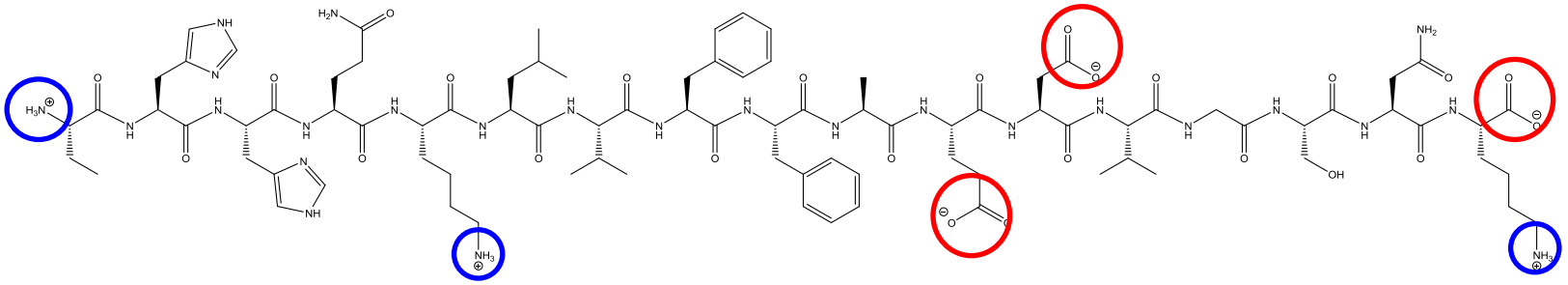

12 15 20 25 28

B

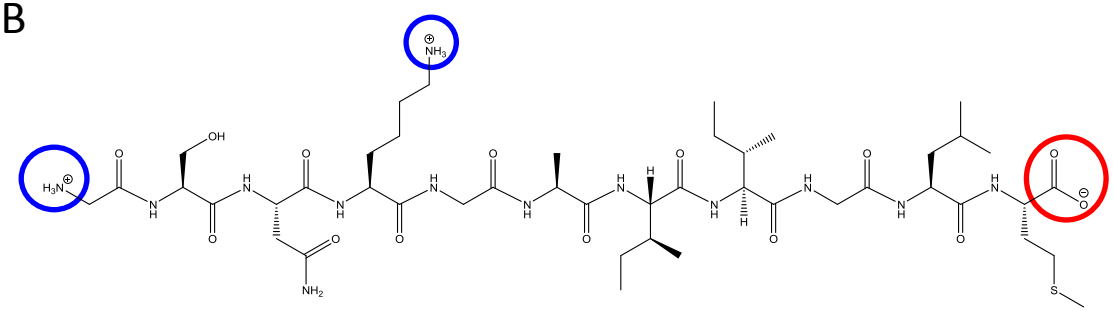

25 30 35

Figure 2

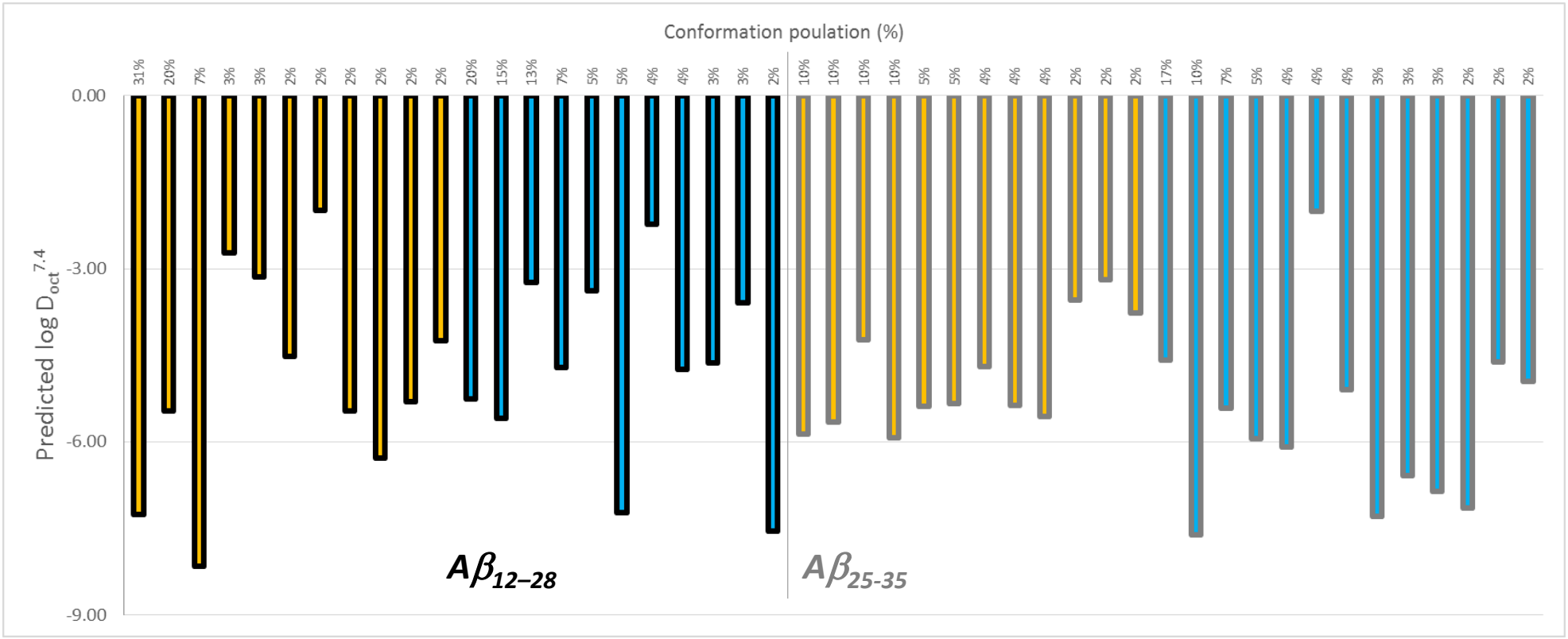
Conformation poulation (%)
31% 20% 7% 3% 3% 2% 2% 2% 2% 2% 2% 20% 15% 13% 7% 5% 5% 4% 4% 3% 3% 2%
10% 10% 10% 10% 5% 5% 4% 4% 4% 2% 2% 2% 17% 10% 7% 5% 4% 4% 4% 3% 3% 3% 2% 2% 2%
0.00
-3.00
-6.00
-9.00
Predicted log $D_{oct}^{7.4}$
$A\beta_{12-28}$
$A\beta_{25-35}$

Figure 3

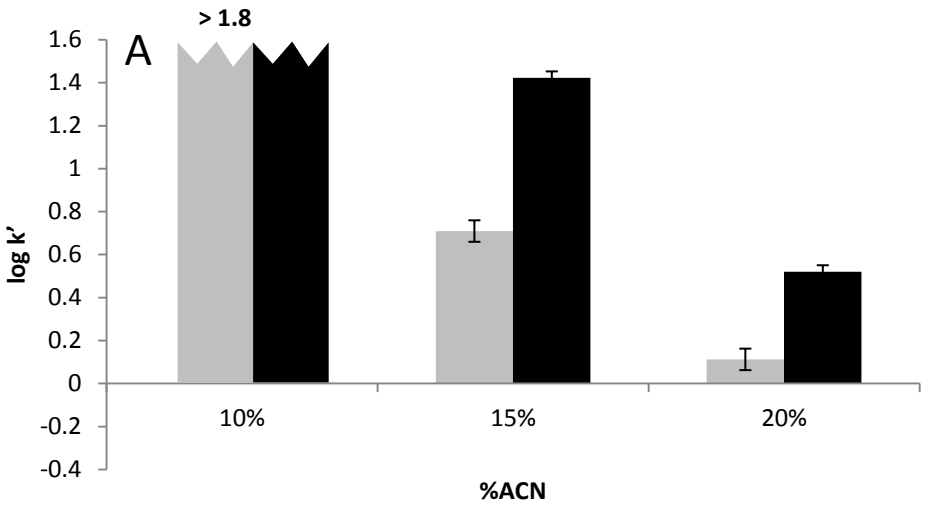
A
> 1.8
1.6
1.4
1.2
1
0.8
0.6
0.4
0.2
0
-0.2
-0.4
log k'
10%
15%
20%
%ACN

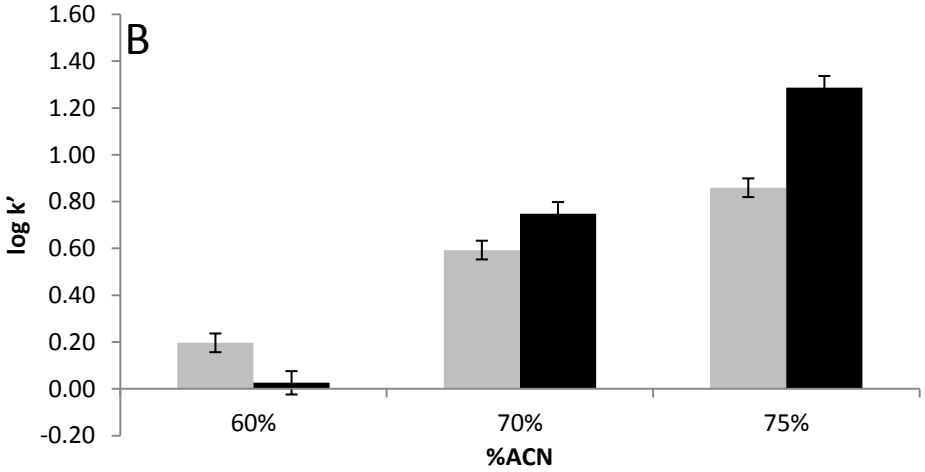
B
1.60
1.40
1.20
1.00
0.80
0.60
0.40
0.20
0.00
-0.20
log k'
60%
70%
75%
%ACN

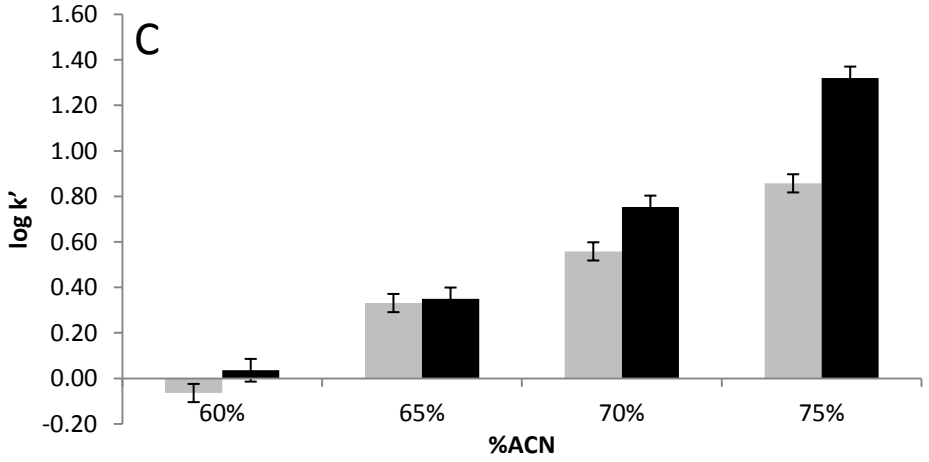
C
1.60
1.40
1.20
1.00
0.80
0.60
0.40
0.20
0.00
-0.20
log k'
60%
65%
70%
75%
%ACN

Figure 4

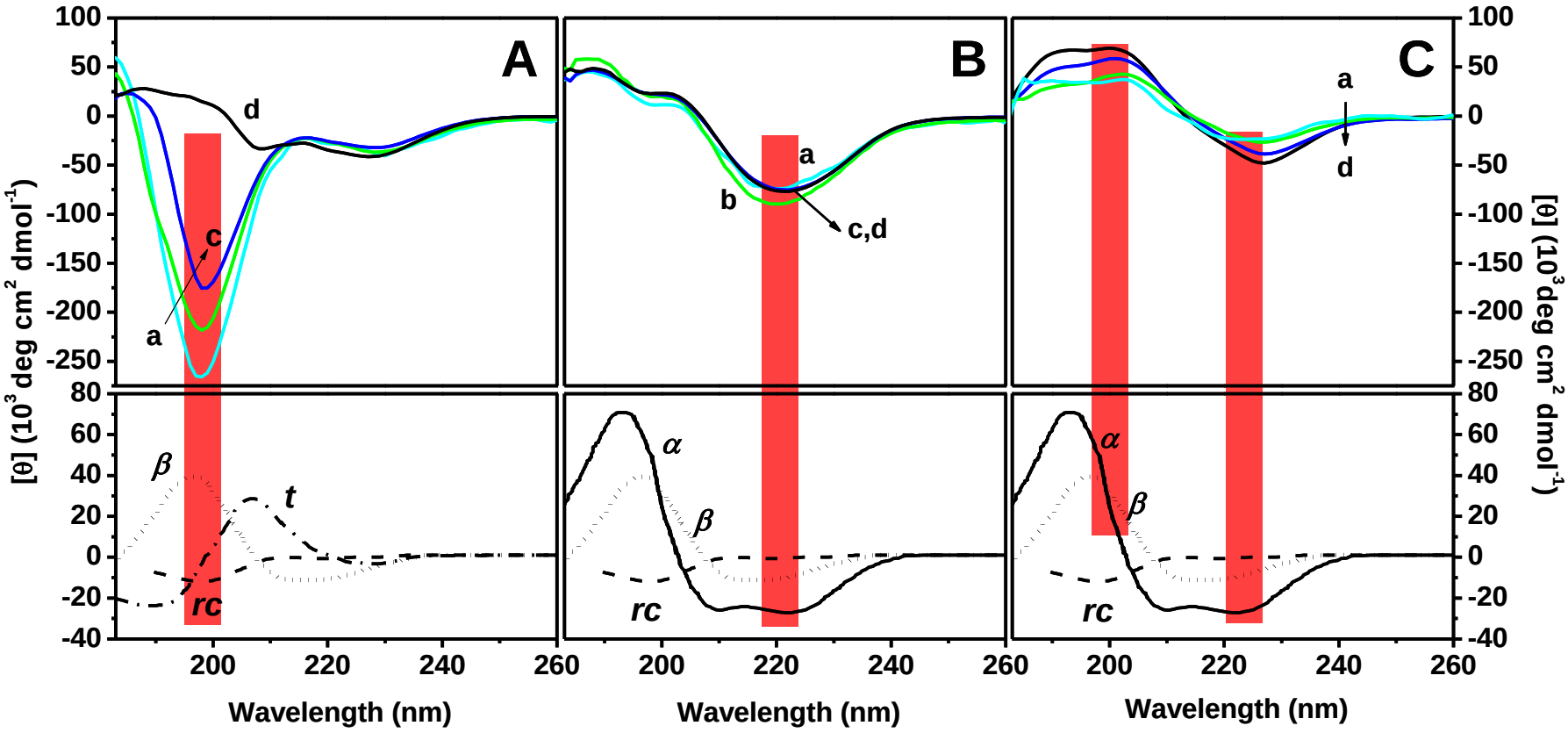
A
B
C
a
b
c
d
c,d
β
t
rc
α
[θ] (10³deg cm² dmol⁻¹)
Wavelength (nm)
100
50
0
-50
-100
-150
-200
-250
80
60
40
20
-20
-40
200
220
240
260

Figure 5

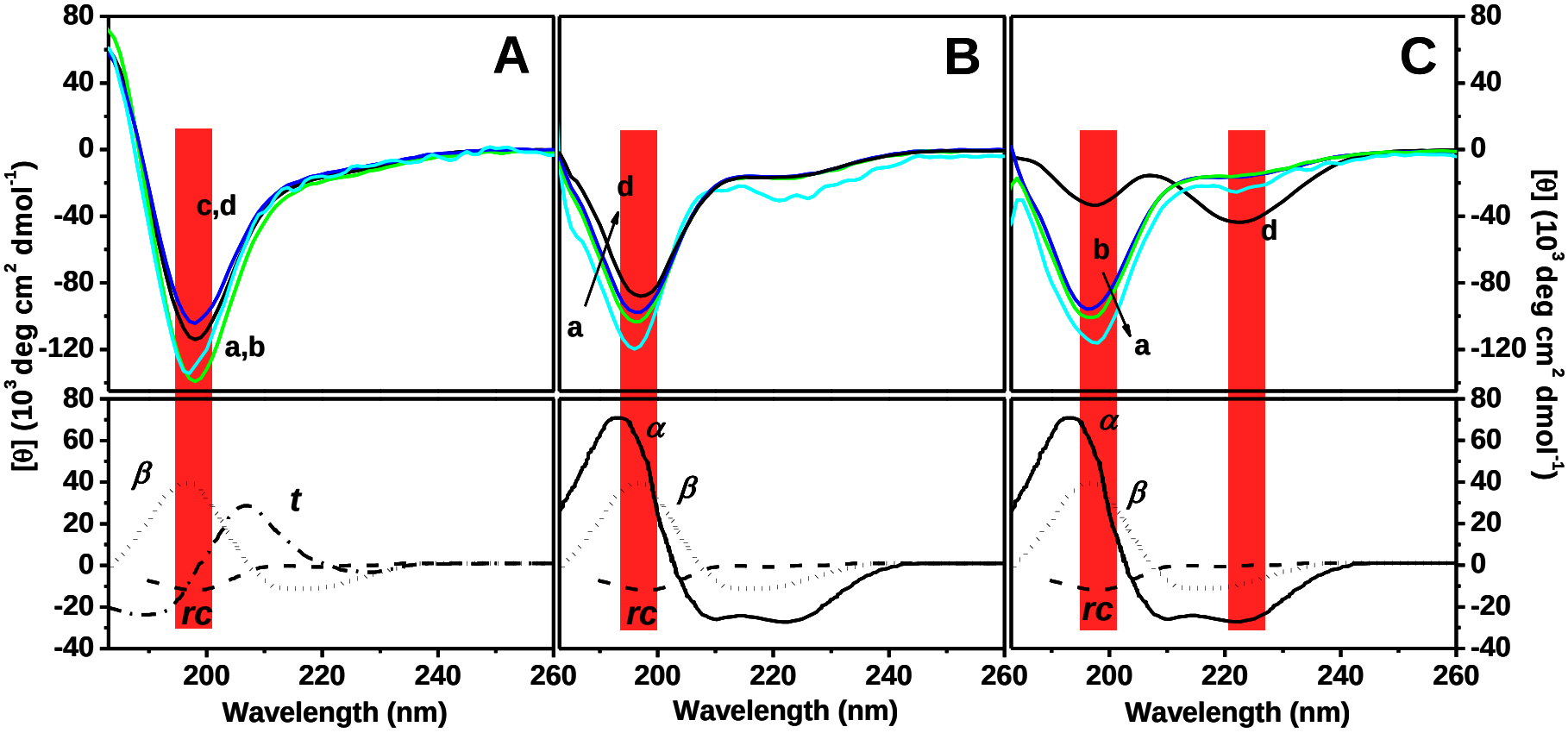
A
B
C
c,d
a,b
d
a
b
a
d
β
t
rc
α
β
rc
α
β
rc
[θ] (10³ deg cm² dmol⁻¹)
[θ] (10³ deg cm² dmol⁻¹)
Wavelength (nm)
Wavelength (nm)
Wavelength (nm)

Supplementary Material

Click here to download Supplementary Material: gcaron_ijp_SupplementaryMaterial.docx